Environment International 183 (2024) 108372

Contents lists available at ScienceDirect

Environment International

journal homepage: www.elsevier.com/locate/envint

Full length article

Exposure to the environmentally relevant fungicide Maneb: Studying toxicity in the soil nematode *Caenorhabditis elegans*

Laura Kubens [a,b], Ann-Kathrin Weishaupt [a,c], Vivien Michaelis [a], Isabelle Rohn [d], Fabian Mohr [b], Julia Bornhorst [a,c,*]

[a] *Food Chemistry, University of Wuppertal, Germany*
[b] *Inorganic Chemistry, University of Wuppertal, Germany*
[c] *TraceAge – DFG Research Unit on Interactions of Essential Trace Elements in Healthy and Diseased Elderly (FOR 2558), Berlin-Potsdam-Jena-Wuppertal, Germany*
[d] *Food Chemistry, University of Potsdam, Germany*

ARTICLE INFO

Handling Editor: Adrian Covaci

Keywords:
Maneb
Fungicide
Manganese
Caenorhabditis elegans
Neurotoxicity
Oxidative stress

ABSTRACT

Maneb is a manganese-containing ethylene bisdithiocarbamate fungicide and is still commonly used as no cases of resistance have been documented. However, studies have shown that Maneb exposure has neurodegenerative potential in mammals, resulting in symptoms affecting the motor system. Despite its extensive use, structural elucidation of Maneb has only recently been accomplished by our group. This study aimed to examine the bioavailability of Maneb, the quantification of oxidative stress-related endpoints and neurotransmitters employing pure Maneb, its metabolites and structural analogues, in the model organism *Caenorhabditis elegans*. Exposure to Maneb did not increase the bioavailability of Mn compared to manganese chloride, although Maneb was about 8 times more toxic with regard to lethality. Maneb generated not significantly reactive oxygen and nitrogen species (RONS) but decreased the ATP level while increasing the amount of glutathione and its oxidized form in a dose-dependent manner. Nevertheless, an alteration in the neurotransmitter homeostasis of dopamine, acetylcholine, and gamma-butyric acid (GABA) was observed as well as morphological changes in the dopaminergic neurons upon Maneb exposure, which underlines the assumption of the neurotoxic potential of Maneb. This study showed that Maneb exhibits effects based on a combined interaction of the ligand and manganese.

1. Introduction

Polymeric ethylene bisdithiocarbamate (EBDC) containing fungicides and their salts were patented in the 1940s as the first broad-spectrum foliar fungicides (Hester and Hill, 1943). In 1950 the manganese (Mn) containing EBDC fungicide was patented and marketed under the brand name Maneb (MB) (Flenner, 1950). Since then, it has been widely used in over 100 different crops, including potatoes, tomatoes, and bananas (Caldas et al., 2004; Thind and Hollomon, 2018). Because EBDC-based fungicides have a highly effective multi-site mode of action, they are commonly used in mixtures with other fungicides as part of resistance management strategies (Thind and Hollomon, 2018). Since this class of fungicides does not act systemically in the plant and is used preventively, they have to be repeatedly applied, which increases the amount of active ingredient entering the environment. Occasionally, exact molecular structures of compounds known for ages remain unknown, this is also true for MB. Its molecular structure was unknown for over 70 years and has only recently been elucidated by our group (Kubens et al., 2023). Contrary to expectations, MB is very stable towards oxidation in the solid-state due to a two-dimensional polymeric network structure with intramolecular sulfur bridges. In dimethylsulfoxide (DMSO) solution MB forms a coordination polymer with two coordinating DMSO molecules in each unit cell (Kubens et al., 2023). MB is thus a polymer of unknown length and its insolubility makes it unsuitable for conventional liquid chromatography coupled with mass spectrometry. Therefore, residue analyses of dithiocarbamate (DTC)-containing fungicides in crops are based on carbon disulfide (CS_2) content and do not refer to the specific metal species, which makes it impossible to distinguish between approved and non-approved EBDC fungicides. The European Food Safety Authority (EFSA) published in their annual report on pesticide residues from 2020 that the chronic dietary exposure (expressed in % of the acceptable daily intake (ADI)) was between 9 % and 83 %, over all DTC-containing fungicides. Most chronic exposures from other pesticides are typically less than 10 % or

* Corresponding author at: Food Chemistry, University of Wuppertal, Germany.
E-mail address: bornhorst@uni-wuppertal.de (J. Bornhorst).

https://doi.org/10.1016/j.envint.2023.108372
Received 8 August 2023; Received in revised form 2 December 2023; Accepted 4 December 2023
Available online 6 December 2023

even less than 1 % of the ADI. The primary food contributors were apples, pears, and broccoli (Carrasco Cabrera and Medina Pastor, 2022). Thus, the group of dithiocarbamates repeatedly attracts attention due to cases of increased residue levels. Unlike food samples, environmental samples are collected less frequently. Data on possible ecological accumulation of the metals released from EBDC fungicides, especially in soil or water samples, is somewhat limited, and their fate in the environment has not been identified. On the one hand, Mn is a necessary cofactor for several enzymes and is involved in different processes, including metabolism, antioxidant defense, development, and reproduction (Aschner and Aschner, 2005). On the other hand, despite being essential, a chronic over-supply of Mn can lead to neurodegenerative damage with symptoms similar to Parkinson's disease, termed "manganism" (Aschner et al., 2009; Calne et al., 1994; Olanow, 2004).

Various EBDC degradation products are known, including CS_2 and ethylene thiourea (ETU), which is formed by metabolism but also appears as a manufacturing by-product (Camoni et al., 1988). The proposed mode of action of the fungicidal activity is based on disruption of several metabolic processes in fungi by interactions with amino acids, thiol-containing biomolecules or metals from metalloenzymes (Roede and Jones, 2014; Adeyemi and Onwudiwe, 2020). Due to the broad mechanism of action, it can be assumed that this class of fungicides acts non-specifically against fungi and may also affect other organisms and humans. In the 1980 s, a relationship between chronic MB exposure and the development of neurological symptoms in field workers was observed (Ferraz et al., 1988; Israeli et al., 1983; Meco et al., 1994). ETU exposure is associated with chronic effects such as thyroid issues and the risk of thyroid cancer (Hurley, 1998; International Agency for Research on Cancer, 1974). Therefore, occupational or environmental exposure is even more of a concern than dietary intake. Particularly, field workers and residents living close to agriculturally used areas are affected, since these EBDC-containing fungicides are usually applied via aerial spraying. There is epidemiological evidence that exposure to maneb is an environmental risk factor for neurotoxicity. In those studies an association between exposure to MB or the Zn- and Mn-containing Mancozeb (MZ) and elevated hair and blood Mn-levels, as well as ETU in urine was observed (van Wendel de Joode et al., 2014; van Wendel de Joode et al., 2016; Mora et al., 2018). Especially urinary ETU levels are commonly used as an established biomarker for EBDC exposure. An epidemiological study by van Wendel de Joode et al. in Costa Rica among pregnant women found ETU urine concentrations exceeding the U.S. EPA (U.S. Environmental Protection Agency, 1991) reference dose (van Wendel de Joode et al., 2014). One sample even exhibited an acutely high urine concentration, surpassing the study's median ETU concentration by a factor of 100 (van Wendel de Joode et al., 2014). Other studies by van Wendel de Joode et al. (2016) and Mora et al. (2018) indicate that especially children and infants, without fully developed nervous system, may have adverse effects in their neurodevelopment when exposed to EBDC-fungicides (van Wendel de Joode et al., 2016; Mora et al., 2018). Costello et al. (2009) reported in their case-control study in California that exposure to MB and Paraquat within 500 m of the home increased the risk for Parkinson's disease by 75 % (Costello et al., 2009).

In vivo and *in vitro* studies revealed that Mn-containing EBDC exposure caused toxic effects on the cellular level similar to ionic Mn(II) overexposure. These include accumulation of Mn (Carmona et al., 2014; Hoffman et al., 2016), neurotoxic effects (Zhou et al., 2004; Kurzatkowski and Trombetta, 2013; Domico et al., 2006; Liu et al., 2023), and alteration in the glutathione (GSH) antioxidant system (Barlow et al., 2005; Domico et al., 2006; Paganotto Leandro et al., 2021) as a marker for oxidative stress.

Due to the fact that most toxicological studies of MB use the fungicide either as a formulation with various additives, pesticide standards, or the less well characterized MZ, this study focused on the effect of pure, synthesized MB (Kubens et al., 2023). However, it has not yet been determined if the toxicity of MB is primarily caused by the fungicide itself, the released ionic Mn, the organic EBDC backbone, its degradation products or a combined effect. Therefore, this study addressed the toxicological effects of MB in comparison to $MnCl_2$, the trace element-free EBDC disodium salt Nabam (NB) and the major EBDC-metabolite ETU using the wild-type nematode *Caenorhabditis elegans* (*C. elegans*) as an *in vivo* model organism. Mechanistically relevant endpoints as for oxidative stress and neurotoxicity were assessed in this study by an unequivocal quantification of the respective molecules by recently established highly sensitive instrumental analytical methods (Weishaupt et al., 2023, Thiel et al., 2023).

C. elegans is a transparent nematode that lives in organic-rich soils in temperate environments and is directly affected by applied pesticides. *C. elegans* has a rapid lifecycle and provides a self-fertilizing hermaphrodite with many offspring using *Escherichia coli* (*E. coli*) as a food source. *C. elegans* also features a fully sequenced genome with many homologs to the mammalian system (Brenner, 1974; C. elegans Sequencing Consortium (1998): Genome sequence of the nematode *C. elegans*: a platform for investigating biology). For example, the nematode features genes involved in trace metal homeostasis and their transporters, allowing investigations of trace metal-induced toxicity (Chen et al., 2013; Martins et al., 2022). Because of its numerous properties, the worm is a popular model organism for studying neurotoxicity according to the 3 R-principle (refine, reduce, replace) (Leung et al., 2008; Soares et al.). *C. elegans* features a nervous system with functionality similar to humans and, for example, also secretes neurotransmitters like dopamine (DA), serotonin (SRT), acetylcholine (ACh), gamma-aminobutyric acid (GABA), glutamate and others (Sulston et al., 1975; McIntire et al., 1993; Serrano-Saiz et al., 2013; Pereira et al., 2015; Martins et al., 2022). Furthermore, its transparency enables the observation of GFP-tagged proteins such as the dopamine transporter 1 (DAT-1) in the transgenic *C. elegans* strain BY200 and allows to detect morphological changes in the dopaminergic (DAergic) neurons (Nass et al., 2002). Thus, *C. elegans* is a widely used model for studying neurotoxicity.

In this study, we investigated acute toxic effects of each relevant substance (MB, ionic Mn and the MB derived metabolites) and examined the bioavailability of the individual Mn species in *C. elegans*. We utilized advanced instrumental analytics to quantify neurotransmitter and glutathione levels along with energy-related nucleotides. These finding were complemented by visualizing morphological changes in DAergic neurons.

2. Material and methods

2.1. Caenorhabditis elegans strain and maintenance

C. elegans wild-type (WT) N2 Bristol was obtained from the *Caenorhabditis* Genetics Center (CGC) (Minneapolis, MN, USA) and the BY200 strain [vtls1(*dat-1*p::GFP; *rol-6*)] was obtained from the Aschner Lab (Einstein Center of Toxicology, Albert Einstein College of Medicine, New York). Worm populations were cultivated on 8P plates seeded with the *E. coli* strain NA22 at 20 °C, as described by Brenner in 1974 (Brenner, 1974). All experiments were performed in synchronized L1 stage larvae. According to standard protocols, age-synchronized worm populations were obtained using a bleach solution (1 % sodium hypochlorite, 0.25 M NaOH). The released eggs were purified by centrifugation with a sucrose solution and worms were allowed to hatch overnight in M9 buffer.

2.2. Materials and synthesis

Manganese(II) chloride ($MnCl_2{\cdot}4H_2O$, 99.99 % trace element basis) was obtained from Sigma-Aldrich. The fungicide MB was synthesized as previously published and characterized *via* elemental analysis, thermal gravimetric analysis, X-ray diffraction, X-ray absorption studies, and electron diffraction (Kubens et al., 2023). Ethylene thiourea (ETU) was supplied from Sigma Aldrich. Stock solutions of each substance were prepared immediately before each experiment. For $MnCl_2$, a 2 M stock

solution in 85 mM NaCl was maintained at 4 °C for up to 6 weeks, and the corresponding working solution was diluted fresh daily. The sodium-containing structural analog NB was synthesized as described in the supplementary material (Klöpping and van der Kerk, 1951).

2.3. Acute exposure

For all experiments 60,000 synchronized L1 larvae were exposed in the absence of *E. coli* for up to 2 h at different concentrations in a volume of 6 mL (resulting in "worm concentration" 10 k/mL). In the case of the water-insoluble fungicide MB, each concentration contained 2 % dimethyl sulfoxide (DMSO, >99.8 % p.a., Roth); therefore, a vehicle control with 2 % DMSO was included in each experiment. Exposure intervals of 30 min and 2 h were chosen to investigate acute effects on L1 larvae. For some studies, 4,000 exposed L1 worms were transferred on nematode growth medium (NGM) plates coated with the *E. coli* strain OP50, allowing them to reach the L4 larvae stage.

2.4. Survival assay

Following treatment, nematodes were washed three times with 85 mM NaCl. The lethality of the substances was determined using the survival assay (Bornhorst et al., 2014). Approximately 30 to 40 L1 larvae per condition (in triplicate) were pre-counted and transferred to coated NGM plates. 48 h post-exposure, the number of surviving worms was scored as a percentage of the original worm count to evaluate the survival rate.

2.5. Measurement of Mn bioavailability

Mn bioavailability of the species was determined in 60,000 L1 stage worms using inductively coupled plasma-optical emission spectrometry (ICP-OES) (Avio 220 Max, Perkin Elmer). The samples were homogenized on ice to prevent protein denaturation (3x freeze–thaw cycles and sonication (3 × 20 s, 1 cycle, 100 % amplitude). After centrifugation (10 min, 10.000 rpm, 4 °C), an aliquot of the supernatant was collected for protein determination. Subsequently, the worm suspension was dried and then acid-assisted digested (HNO_3/H_2O_2, 1:1, suprapure® 65 % nitric acid, 30 % hydrogen peroxide, Merck) overnight at 95 °C. Ashed samples were re-suspended in 1 mL of 2 % HNO_3 with Yttrium (10 µg/L, single element ICP standard, Roth) as internal standard and diluted 1:3 for ICP-OES measurements. The instrument settings were chosen as follows: plasma power 1500 W, plasma gas flow: 10 L/min, auxiliary gas flow 0.2 L/min, nebulizer gas flow: 0.70 L/min, pump flow rate: 1 mL/min, Wavelength: Mn 257.610 nm, Y 371.029 nm. An external calibration was prepared using a multi-element mix (Inorganic Ventures) for evaluation. Mn amounts were validated by measuring acid-assisted digested certified reference material (BCR-274, single cell protein, Institute for Reference Materials and Measurement of the European Commission, Geel, Belgium) and reference water (SRM-1640a, trace elements in natural water, National Institute of Standards and Technology, Gaithersburg, MD, USA).

2.6. Protein determination via bicinchoninic acid (BCA) assay

All analytical data were normalized to protein content, including total Mn bioavailability, neurotransmitter, and GSH/GSSG levels. The protein amount was determined using the bicinchoninic acid (BCA) assay (Sigma Aldrich) with bovine serum albumin (Sigma Aldrich) (100 to 1000 µg/mL) as an external calibration standard. The BCA assay was performed according to standard protocols (Smith et al., 1985) and absorption was measured at 560 nm using a microplate reader (Infinite M Plex, Tecan).

2.7. Neurotransmitter quantification

Neurotransmitter levels were quantified according to a method using LC-MS/MS and deuterated standards of DA, SRT, ACh, and GABA, which has been previously published (Weishaupt et al., 2023). 60,000 L1 worms were exposed to the respective compounds for 2 h and washed three times with 85 mM NaCl solution. 4,000 L1 worms of each treatment condition were seeded on OP50 *E. coli*-coated NGM plates and allowed to reach the L4 larvae stage. L1 worms were immediately shock-frozen in liquid nitrogen and L4 stage larvae were pelleted after 48 h resting. Pellets were stored at −80 °C, and sample preparation was performed as described previously.

2.8. Fluorescence microscopy of DAergic neurons

The BY200 strain (Nass et al., 2002) was exposed for 2 h during L1 larval stage according to the described exposure procedure. For imaging both larval stages (L1 and L4-stage (48 h post-treatment)), worms were carefully transferred onto 4 % agarose pads and anesthetized with 5 mM levamisole. Images were acquired using a Leica DM6 B Fluorescence Microscope equipped with a x63 magnification lens. Fluorescence images were captured with excitation at 460–500 nm and an emission range of 512–542 nm. The following parameters were selected: For L1 worms using the 63x magnification lens: 500 ms exposure time for both modes. For L4 worms using the 63x lens: 750 ms brightfield, 275 ms fluorescence. A series of z-stacked (20 steps) was obtained by optical sectioning at approximately 0.5 µm intervals. Images were processed and edited using the thunder function (small volume computational cleaning, adaptive strategy (water) of the LAS X (Leica) software. This procedure aimed to obtain blur-free detailed overlays. For evaluation the following modified (Bijwadia et al., 2021; Baesler et al., 2021) scoring system was chosen: 1 = no alterations visible, 2 = irregular dendrites (kinks, bends), 3 = blebbing (Chen et al., 2011) ("beads on a string"), 4 = loss of dendrites or/and shrunken soma, 5 = loss of dendrites or/and loss of soma. To ensure the identification morphological abnormalities, 6-hydroxydopamine was used as a positive control (L1 stage worms were exposed for 2 h with 5 mM) (Nass et al., 2002).

2.9. Carboxy-DCFH-DA-assay for RONS measurement

The formation of reactive oxygen and nitrogen species (RONS) was determined by a 6-carboxy-2′,7′-dichlordihydrofluorescein-diacetate (carboxy-DCFH-DA)-based fluorescence emission assay (Bornhorst et al., 2014). A 50 mM carboxy-DCFH-DA stock solution in DMSO was prepared immediately before the experiment. 50,000 synchronized L1 worms were exposed to 500 µM carboxy-DCFH-DA for 1 h in the dark. After treatment, the worms were washed with M9 buffer and three times with 85 mM NaCl. Subsequently, 8,000 L1 worms were transferred to each well in a 96-well plate and incubated with 350 µM *tert*-butyl hydroperoxide (*t*-BOOH) as a RONS generating positive control, different MB and $MnCl_2$ concentrations, as well as NB and ETU in triplicate. The cellular oxidation of carboxy-DCFH was monitored immediately (excitation: 485 nm, emission: 520 nm) by a microplate reader (Infinite M Plex, Tecan, Switzerland), and measurements were conducted every 30 min up to 4 h. Data were normalized to carboxy-DCFH-DA treated controls or, in case of MB, to the carboxy-DCFH-DA treated DMSO-vehicle controls.

2.10. Adenine nucleotide quantification

Adenine nucleotides (ATP, ADP, AMP) were quantified as described in (Neumann et al., 2020) with minor modifications. 100,000 exposed L1 stage worms were extracted by adding 150 µL 0.5 M KOH and homogenizing for 40 s, followed by neutralization with 30 µL phosphoric acid (10 %). The nucleotides were measured by an Agilent 1260 Infinity II System equipped with a DAD detector Agilent 1315C.

2.11. GSH and GSSG quantification

The total glutathione (GSH) and glutathione disulfide (GSSG) levels were evaluated according to a previously published method using N-ethylmaleimide (NEM) bound GSH as well as GSSG for external calibration (Thiel et al., 2023). Exposure of L1 worms was conducted as described in the neurotransmitter quantification section and samples were prepared as described.

2.12. Statistical analysis

All data were analyzed and plotted using GraphPad Prism 6 (GraphPad Software, La Jolla, CA, USA). Data are shown as means with standard error of the mean (SEM). The used statistical test to compare concentrations and species to their respective controls are stated below each figure.

3. Results and discussion

3.1. Acute toxicity

Many studies indicate that MB has a toxic potential, especially its role in neurotoxicity and induction of oxidative stress is discussed (Anderson et al., 2021; Barlow et al., 2005; Liu et al., 2023). Mn has also been attributed to cause impaired dopaminergic, glutamatergic, and GABAergic transmission, oxidative stress and mitochondrial dysfunction (Tuschl et al., 2013). However, no direct comparison of MB, ionic Mn and the MB derived metabolites in one model organism were carried out with respect to toxicity. Therefore, as a first step, the toxicity of MB in *C. elegans* after acute exposure was compared with that of $MnCl_2$, NB, and ETU. Since commercially available pesticide standards can vary significantly in quality and the exact molecular structure of MB has just recently been reported, it was synthesized as previously published (Kubens et al., 2023). Previous studies either used MB in a formulation with other additives or pesticide standards. However, in order to specifically investigate the effect of the active ingredient, the existence of a pure substance is of critical importance. NB was also synthesized and obtained as a hexahydrate (Klöpping and van der Kerk, 1951).

The dose–response survival curve revealed significant toxic effects induced by MB. It decreased survival rates in a dose-dependent manner, with an LD_{50} (dose which is lethal for 50 % of a tested population) of approximately 0.6 mM after 2 h exposure (Fig. 1). Compared to $MnCl_2$ with an LD_{50} of 5 mM, MB appears to be about eight times more toxic (Table 1). These findings agree with an *in vitro* study comparing MB to several Mn species in PC12 rat pheochromocytoma cells (Carmona et al., 2014).

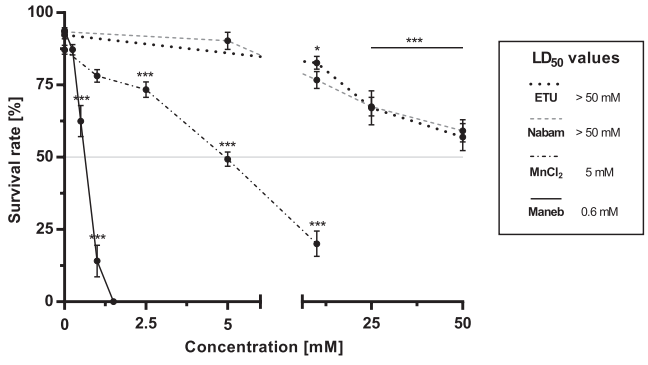

Fig. 1. Dose-response curves following acute exposure to Maneb (MB), $MnCl_2$, Nabam (NB), and ETU. In the box the respective LD_{50} values are shown. N2 (wild-type, WT) worms were treated for 2 h at the L1 larvae stage with increasing concentrations of different compounds. Data are expressed as means ± SEM from at least four independent experiments (each experiment with three replicates). A one-way ANOVA with a Dunnett's multiple comparisons test was used for the statistical analysis. Following *p*-value summary was chosen: *p < 0.05, **p < 0.01, ***p < 0.001 compared to untreated control.

Table 1
Total Mn content of *C. elegans* wild-type L1 worms measured with ICP-OES following 2 h incubation with the respective Mn species. Data are expressed as means ± SEM of at least five independent experiments. The individual LD_{50} dose is printed in bold. For control, a mean (n = 26) was built of non-treated worms in 85 mM NaCl and non-treated worms with 2 % DMSO as vehicle control.

	Concentration [mM]	Total Mn ± SEM [ng Mn/µg protein]	
Control	0	0.15 ± 0.01	x- fold of control
Maneb	0.1	0.25 ± 0.01	1.7 x
	0.25	0.38 ± 0.03	2.6 x
	0.5	**0.88 ± 0.15**	**6.0 x**
$MnCl_2$	0.1	0.38 ± 0.03	2.6 x
	0.25	0.58 ± 0.03	4.0 x
	0.5	0.94 ± 0.12	6.4 x
	5	**4.8 ± 0.4**	**33 x** *

* 5.5-fold higher Mn content compared to LD_{50} of Maneb.

In contrast, the disodium salt NB and the primary metabolite ETU showed no significant effects in the same concentration range (0 to 5 mM). Both showed increased toxic effects only at concentrations greater than 10 mM, but even at the highest applied dose of 50 mM, a lethality of 50 % was not reached. These effects are consistent with cytotoxicity results from the literature (Cova et al., 1991; Domico et al., 2006). Since several studies have shown *in vitro* that MB exposure leads to higher cytotoxicity than NB, ETU, and $MnCl_2$, it was suggested that the complexed Mn in MB might be more bioavailable. Consequently, all subsequent experiments in this study were performed at subtoxic concentrations, including 0.1 mM and 0.25 mM for MB and 0.25 mM and 0.5 mM for $MnCl_2$ and their respective LD_{50} concentrations. In the case of NB and ETU, the subtoxic concentration of 5 mM was chosen as the highest concentration of the Mn-species range (5 mM).

3.2. Bioavailability of Mn

To investigate if the increased lethality of MB might be the result of an increased bioavailability of Mn, the total amount of Mn in L1 stage worms after acute treatment was quantified using inductively coupled plasma-optical emission spectrometry (ICP-OES). Treatment with higher doses for both Mn species increased total Mn time- and concentration-dependent (30 min *vs.* 2 h, Fig. 2. (**A**)). A comparison of the total Mn amount after 2 h exposure to a subtoxic concentration showed that the more toxic MB species accumulated to a lower extent than the less harmful $MnCl_2$ (Fig. 2 (**B**)). For example, incubating 0.1 mM or 0.25 mM of MB for 2 h resulted in a 1.5-fold lower total Mn level than $MnCl_2$ at the same dose (Table 1). Thus, the data suggest an inverse relationship between toxicity and Mn bioavailability of the species.

Moreover, the total amount of Mn at the LD_{50} concentration was about five times higher in the case of $MnCl_2$ compared to MB. To determine if Mn is still present in the L4-stage worms, treated and non-treated L1 larvae were placed on NGM plates for 48 h post-exposure. Total Mn content in the L4 animals was also determined *via* ICP-OES but no difference was found compared to untreated control nematodes indicating an elimination of Mn once treatment ended (Figure S4). NB and ETU-treated samples were also quantified, but as expected, Mn levels were not altered (data not shown).

Bioavailability data of $MnCl_2$ are in agreement with data of Peres et al., exposing L1 stage worms for 1 h (Peres et al., 2018). Carmona et al. also observed an approximately 10-fold higher cytotoxicity of MB *in vitro* in PC12 rat pheochromocytoma cells compared to other Mn species. As in our study, no species-specific differences in Mn bioavailability was found (Carmona et al., 2014).

Based on the bioavailability results, it was concluded that the higher toxicity of MB may not be caused by overexposure to Mn alone. Therefore, more detailed mechanistic studies were performed.

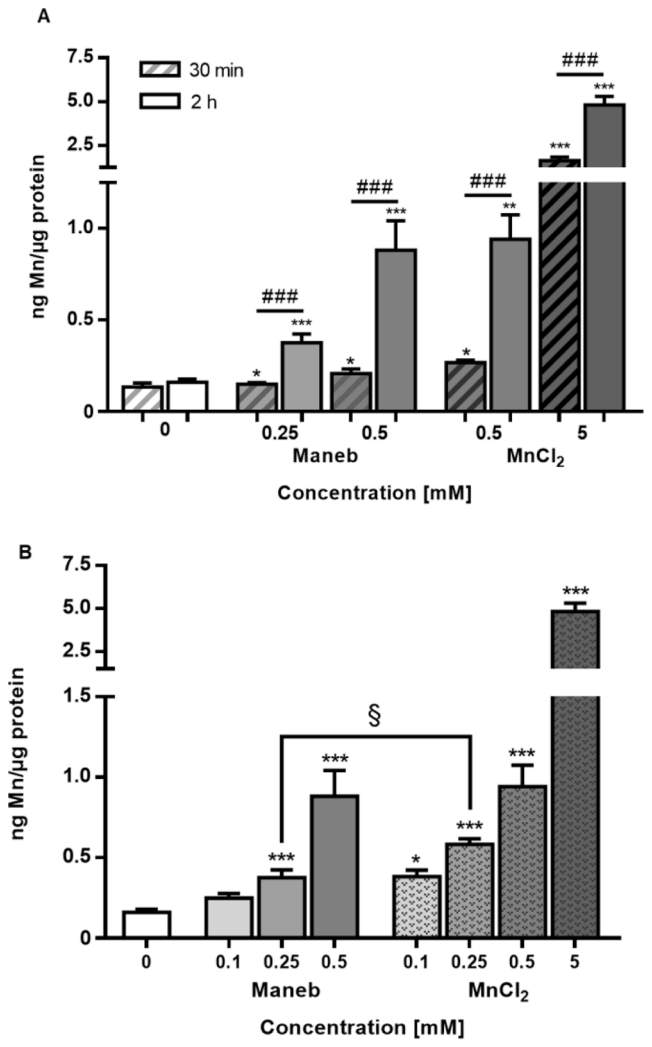

Fig. 2. (A) Mn contents following Maneb and $MnCl_2$ exposure (time- and concentration-dependent). Total Mn amount (normalized to protein content) of wild-type worms (L1 larvae) following acute Maneb or $MnCl_2$ exposure at two different exposure times. Data are expressed as means ± SEM from at least three (30 min n = 3, 2 h: n = 5) independent experiments. (**B**) Species-specific effects. Total Mn amount (normalized to protein content) of wild-type worms (L1 larvae) following acute Maneb or $MnCl_2$ exposure for 2 h. Data are expressed as means ± SEM from at least five independent experiments. A two-way ANOVA with a Tukey's multiple comparisons test was used for the statistical analysis. Following *p*-value summary was chosen: *p < 0.05, **p < 0.01, ***p < 0.001 compared to untreated control and §p < 0.05, compared to different species and ###p < 0.001 compared to different exposure time.

3.3. Neurotoxicity

Neurotransmitters (NT) are essential for proper function of the neural system; even small changes in their homeostasis and equilibrium can significantly impact the signaling cascade. Alterations in NT homeostasis are associated with neurodegenerative diseases including Alzheimer's disease, Parkinson's disease (PD), or Huntington's disease (Francis et al., 1999; Hornykiewicz, 2006; Walker, 2007). First, no treatment-related changes in NT levels of L1 or L4 larval stage worms were observed at a concentration of 5 mM NB or ETU (Fig. 3 (**A-D**), Figure S5 (**A-D**)). An MB concentration of 0.5 mM (LD_{50}) leads to a significant decrease in DA, ACh, and GABA levels in L1 larvae compared to the untreated control (Fig. 3 (**A-D**)). For comparison, exposure to $MnCl_2$ at the LD_{50} concentration (5 mM) did not lead to significant changes in DA, SRT or ACh levels at any concentration or larval stage (Fig. 3 (**A-C**), Figure S5 (**A-D**)). GABA levels were significantly decreased at 5 mM $MnCl_2$ in L1 larvae (comparable to the LD_{50} of MB) (Fig. 3 (**D**)). However, after MB exposure the NT level alteration is rather acute since no more long-lasting effects are evident 48 post-treatment in the L4 stage worms (Figure S5 (**A-D**)).

In addition to quantifying neurotransmitter levels, the architecture of the DAergic neurons was assessed by using worms expressing green fluorescent protein (GFP) under the control of a promoter for the dopamine re-uptake transporter 1 (*C. elegans* orthologue for vertebrate DAT 43), pdat-1::GFP (vtIs1). In L1-stage worms, the anterior deirids (ADE) processes (dendrites) and the posterior deirids (PDE) are not yet observable, as they develop between the first and second larval stage (Sulston et al., 1975). However, exemplary L1-worm images are shown in the supplementary material Figure S6, where all four cephalic sensilla (CEP) dendrites of the untreated L1-worm are visibly intact, while worms treated with 0.5 mM Maneb showed less fluorescence intensity in the cell bodies, as well as in the dendrites. Worms exposed to 5 mM 6-OHDA served as positive controls and display frequently occurring abnormalities (Figure S6 (**C**)). Fig. 4 depicts exemplary images of L4-stage worms at 48 h post-exposure to address later occurring morphological changes. In the control group, all four CEP dendrites were visible (overlaying in the z-stack image) and exhibited no irregularities (Fig. 4 A). The worm in Fig. 4 (**B**) was treated with 0.5 mM MB and the four CEP dendrites were present, but several evaluated worms displayed irregular bends and kinks in their dendrites. Additionally, the cell body size and fluorescence intensity of the ADE neurons was decreased to the extent that both ADE neurons were distinctly visible. The positive control (Fig. 4 (**C**)) treated with 5 mM 6-OHDA exhibited the most pronounced effects across all examined worms. These findings are in agreement with Nass et al. (2002), who reported that all three neuron classes respond with different sensitivity to 6-OHDA (CEP > ADE≫PDE) (Nass et al., 2002). However, after MB exposure, the DAergic ADE neurons seem to be the most sensitive neurons. The frequency and classification of observed abnormalities is summarized in Fig. 5.

These findings indicate that MB disrupts the neurotransmitter homeostasis and induces morphological abnormalities in the DAergic neurons of *C. elegans* pointing out its neurodegenerative potential. Epidemiological data demonstrate that MB exposure is associated with a higher risk of Parkinson's disease (PD), especially when exposure occurs at a younger age (Costello et al., 2009). Mancozeb (Mn and Zn containing EBDC fungicide) exposure during pregnancy is associated with adverse neurodevelopmental effects in children living near banana plantations in Costa Rica (Mora et al., 2018; van Wendel de Joode et al., 2016). Many assumptions have been made about the loss of dopaminergic neurons for the underlying mechanism of action and the neurotoxic potential of MB. The underlying mechanisms are still poorly understood. Two *in vitro* studies (Fitzmaurice et al., 2014; Leiphon and Picklo, 2007) demonstrated decreased aldehyde dehydrogenase (ALDH) activities after MB exposure. ALDHs detoxify many reactive aldehydes generated during metabolism or by xenobiotics (Singh et al., 2013). The dopamine monoamine oxidase (MAO) metabolite 3,4-dihydroxyphenylacetaldehyde (DOPAL), which is detoxified by ALDH, is even in physiological concentrations known to be selectively neurotoxic in dopaminergic neurons targeting the mitochondria. ALDH dysfunctions are associated with dopaminergic neurodegeneration and the pathogenesis of PD, which is characterized by the loss of dopaminergic neurons in the *substantia nigra* and the presence of α-synuclein aggregation (Kalia and Lang, 2015).

Mesencephalic cells exposed to MB showed decreased cellular uptake of ^{3}H-labeled DA and ^{14}C-labeled GABA in a dose-dependent manner (Domico et al., 2006). The underlying principle is based on the fact that irreversible neuronal damage is associated with impaired NT uptake (Zeevalk et al., 1995). Domico *et al.* also investigated the effect of the other species NB, $MnCl_2$ and ETU. $MnCl_2$ and ETU exposure in the same concentration range did not alter the DA and GABA uptake; only higher $MnCl_2$ concentrations resulted in decreased DA uptake. At higher

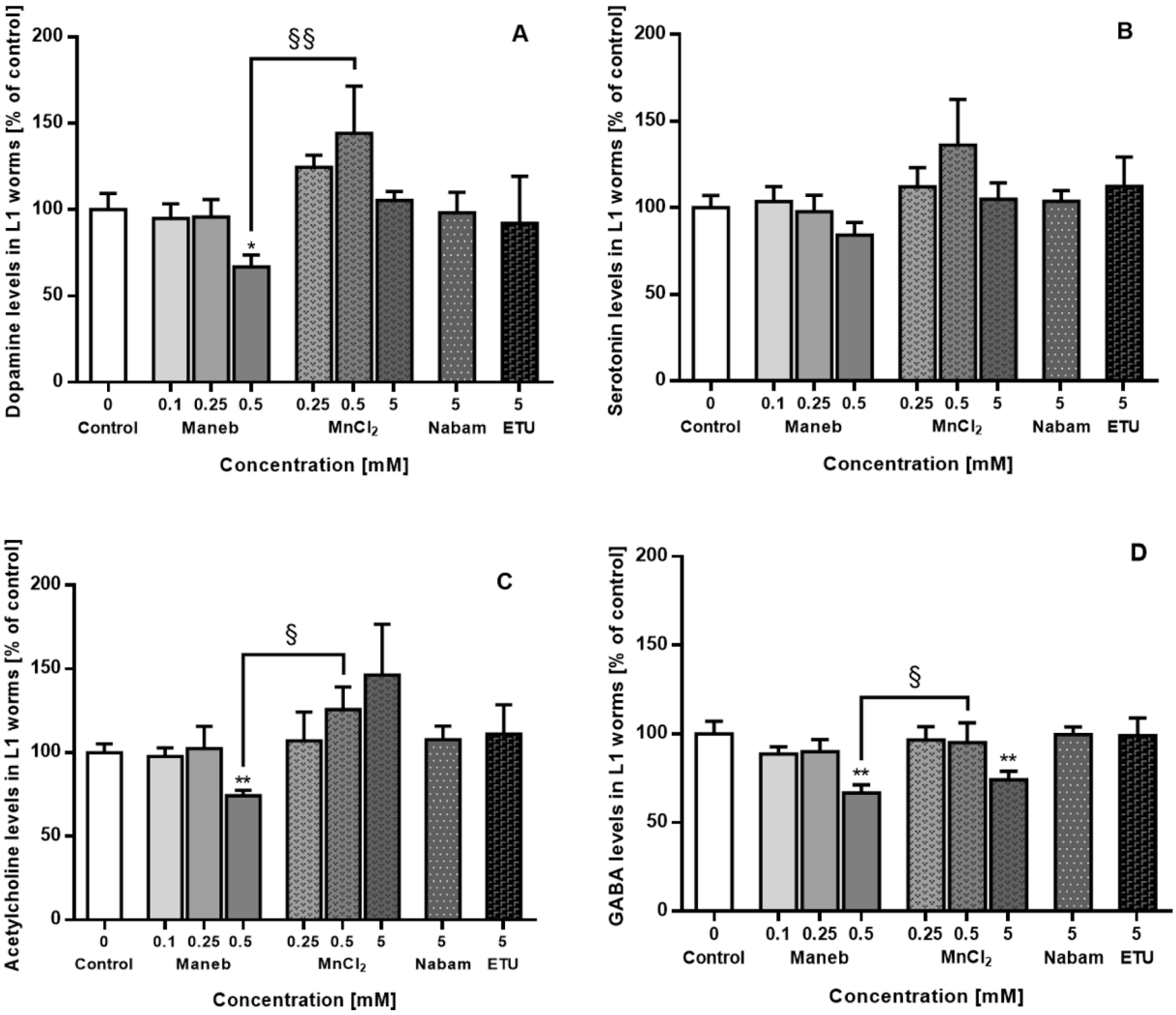

Fig. 3. Neurotransmitter levels (dopamine **(A)**, serotonin **(B)**, acetylcholine **(C)**, GABA **(D)**) measured with LC-MS/MS normalized to protein content and normalized to respective control of wild-type worms (L1 larvae) following acute exposure for 2 h. Data are expressed as means ± SEM from at least three independent experiments. A one-way ANOVA with a Dunnett's multiple comparisons test was used for the statistical analysis. The following *p*-value summary was chosen: *p < 0.05, **p < 0.01 compared to respective untreated control, and §p < 0.05, §§p < 0.01 compared to the same concentration with different species.

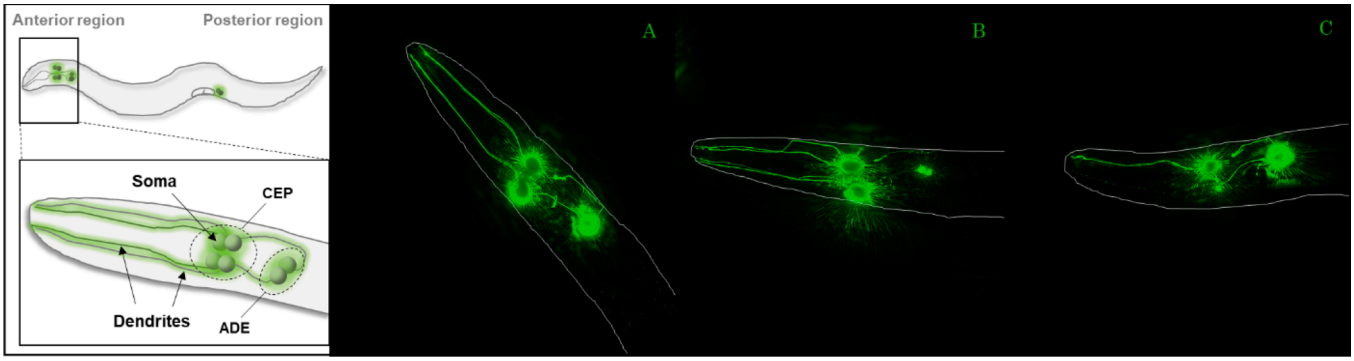

Fig. 4. Visualization and schematic overview of the six dopaminergic neurons (CEP and ADE) in the head (anterior) region in the L4-stage BY200 *C. elegans* strain. Worms were exposed for 2 h in L1-larval stage and the morphology of GFP-expressing DAergic neurons was evaluated in L4-stage, 48 h post-treatment. Shown are combined z-stacked (20 steps) fluorescence images of different conditions: untreated control (**A**), treatment with 0.5 mM Maneb (**B**) and a positive control using 6-OHDA (**C**).

applied concentrations than MB, NB exposure also leads to reduced uptake of both neurotransmitters (Domico et al., 2006). A few studies also investigated the neurotoxic effects of the Mn and Zn-containing EBDC fungicide Mancozeb (MZ) in *C. elegans* (Negga et al., 2011). Experiments showed dopaminergic neurons are most vulnerable to MZ toxicity (Harrison Brody et al., 2013) but also GABAergic neurons seem

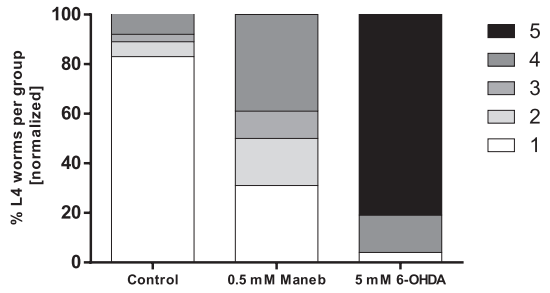

Fig. 5. Percentage distribution of L4 worms assigned to each group (1–5), with each condition normalized to the respective total worm count (approximately 30 worms for each condition were evaluated). *C. elegans* BY200 strain was exposed to the respective species for 2 h in L1-larval stage and analyzed via fluorescence microscopy in L4-stage 48 h post-treatment. The definition of each value was chosen as follows: 1 = no alterations, 2 = irregular dendrites (kinks, bends), 3 = blebbing, 4 = loss of dendrites or/and shrunken soma, 5 = loss of dendrites or/and loss of soma.

affected by MZ exposure (Negga et al., 2012).

NB was generally expected to generate similar effects as a structural analog of MB since both species contain the EBDC backbone. NB is *in vivo* partly metabolized to ETU and about 25 % is excreted *via* urine (Kurttio et al., 1991). During EBDCs metabolizing to ETU, other metabolites such as CS_2 or metal sulfides may be produced, but unmetabolized MB and NB are still present. CS_2 exposure displays many adverse effects, including thyroid disruption, neurotoxicity, and cardiotoxicity (Printemps et al., 2022). However, no alteration was detected in NT levels after NB exposure (Fig. 3 (**A-D**) Figure S5 (**A-D**)). One noticeable difference between the disodium EBDC salt NB and MB is the replacement of Mn^{2+}-ion with two Na^{+}-ions. Moreover, the EBDC ligand acts as monodentate ligand toward Na^{+} ions (Vrábel et al., 1987), while EBDCs in the presence of divalent d-block cations, such as Mn^{2+}, act as bidentate chelate ligands (Hogarth, 2003). In contrast to MB, which is only soluble in coordinating solvents such as DMSO or dimethylformamide, NB is highly water soluble. Although both Mn-EBDC complexes were synthesized in water, the co-crystallizing water molecules of MB dihydrate are not bound to Mn (Kubens et al., 2023). Since the Mn ion prefers soft donor ligands one can assume that when MB enters a biological system, it interacts with sulfur functionalities of cellular molecules including proteins or enzymes (Adeyemi and Onwudiwe, 2020). Furthermore, MB might be more stable than usually assumed in the literature and therefore the toxicological effects might be more related to intact MB rather than its degradation products.

Due to the significant differences in the toxicity of MB and NB, Mn has a considerable influence on the toxicity of MB. However, this Mn-related impact seems to exist only in combination with the organic backbone. Many studies concluded that the mechanism of action is affected by the ability of the ligand to control the reactivity of the metal (Adeyemi and Onwudiwe, 2020). Chronic overexposure of Mn (in the ionic form) in humans can lead to neurodegenerative damage with symptoms similar to Parkinson's disease, termed 'manganism.' The underlying mechanism is not yet fully understood, but it is assumed that Mn accumulates in the brain region *substantia nigra* and leads to the loss of dopaminergic neurons (Aschner et al., 2009). However, in this study only GABA levels decreased in L1 worms after $MnCl_2$ treatment (Fig. 3 (**D**)). Mn complexed to EBDC ligands becomes more lipophilic, implying permeability through cellular membranes (Adeyemi and Onwudiwe, 2020). In addition, another difference in the mechanism of action of the two Mn species might be a different oxidation state since the Mn(II) ions may be oxidized in the cellular environment. Thus, Mn can act as a redox cycler and induce the formation of reactive oxygen and nitrogen species (RONS), resulting in oxidative stress (Chen et al., 2018).

3.4. Reactive oxygen and nitrogen species (RONS) formation and adenine nucleotides

Oxidative stress is the imbalance between reactive species generated by metabolic processes and antioxidant capacity (Halliwell, 2006). Increased amounts of reactive oxygen and nitrogen species (RONS) are associated with several neurodegenerative diseases. However, it is still unclear if RONS are a primary cause or a consequence in the pathogenesis (Andersen, 2004). A further supposed factor involved in the cellular anti-oxidative defense system and promoting cellular oxidative stress are adenine nucleotides. ATP depletion, followed by a decline in cellular energy metabolism is also discussed as underlying mechanism of neurodegenerative diseases as PD or AD (Schon and Przedborski, 2011; Wilson et al., 2023). Therefore, RONS as well as adenine nucleotide levels in the worms were studied upon exposure to MB.

After 30 min and 2 h exposure to MB a slight increase in fluorescence was observed, corresponding to the induction of RONS at higher MB concentrations (Fig. 6 (**A, B**)). Treatment with 0.5 mM MB for 2 h resulted further in a significant decrease of the ATP concentration as well as the total adenylate nucleotide pool (TAN) (Fig. 6 (**C, D**)). However, $MnCl_2$ showed no effect on RONS or ATP at the same concentration (0.5 mM), although bioavailability data revealed similar Mn amounts at concentrations of 0.5 mM compared to both Mn species. However, after exposure to 5 mM $MnCl_2$ a reduced ATP level and depleted TAN was observed. This corroborates previous findings in which exposure to higher $MnCl_2$ concentrations (>5 mM) in *C. elegans* lead to reduced ATP levels (Neumann et al., 2020). Furthermore, exposure to higher $MnCl_2$ concentrations (>5 mM) in *C. elegans* leads to slightly increased RONS levels after 2 h in L1 larval stage (Bornhorst et al., 2014). For MB no data regarding the formation of RONS or an ATP depletion are available in *C. elegans*. However, in human neuroblastoma cells (Liu et al., 2023) MB exposure leads to a concentration-dependent induction of RONS and similar effects were observed after MZ exposure in mesencephalic cells (Domico et al., 2007).

3.5. GSH and GSSG quantification

Oxidative stress is a synonym for the imbalance between reactive species produced by the influence of oxygen and the antioxidant protection systems (Halliwell, 2006). Since only slightly increased RONS levels are generated by MB treatment, the other side of the equilibrium was examined. As a marker for antioxidant capacity the total levels of GSH and GSSG in worm lysates were quantified by using a LC-MS/MS method to determine if MB is affecting the oxidative state as hypothesized. The endogenously synthesized thiol GSH is present in all cells and has many physiological functions, such as its involvement in the antioxidant defense system (Andersen, 2004). MB exposure significantly increased the total GSH levels in L1 stage worms after 2 h exposure in a dose-dependent manner compared to DMSO-treated controls. A maximal increase of total GSH (200 %) was observed for the MB LD_{50} concentration (Fig. 7 (**A**)). However, exposure to any other investigated species did not increase GSH levels. Considering the GSSG levels, the effect of MB becomes even more apparent, as a 10-fold increase (0.5 mM Maneb) was observed compared to the DMSO-treated vehicle control (Fig. 7 (**B**)). These effects are reflected by a decreased GSH/GSSG ratio at 0.5 mM MB exposure (Fig. 7 (**C**)).

MB is thought to interact with thiol groups and might be able to modify protein side chains (Roede and Jones, 2014; Anderson et al., 2021). In a previous *in vitro* study, cells treated with Maneb for 1 h resulted in highly elevated GSSG levels. However, GSH levels were decreased at lower MB concentrations and did not change at higher MB concentration compared to the control (Grosicka-Maciąg et al., 2011). In contrast, in mesencephalic cells an increased level of GSH after Maneb exposure was found, but no changes in the GSSG levels (Barlow et al., 2005). No changes in GSSG levels in the study by Barlow *et al.* could be due to the lack of sensitivity of fluorescent dye-based methods for GSSG

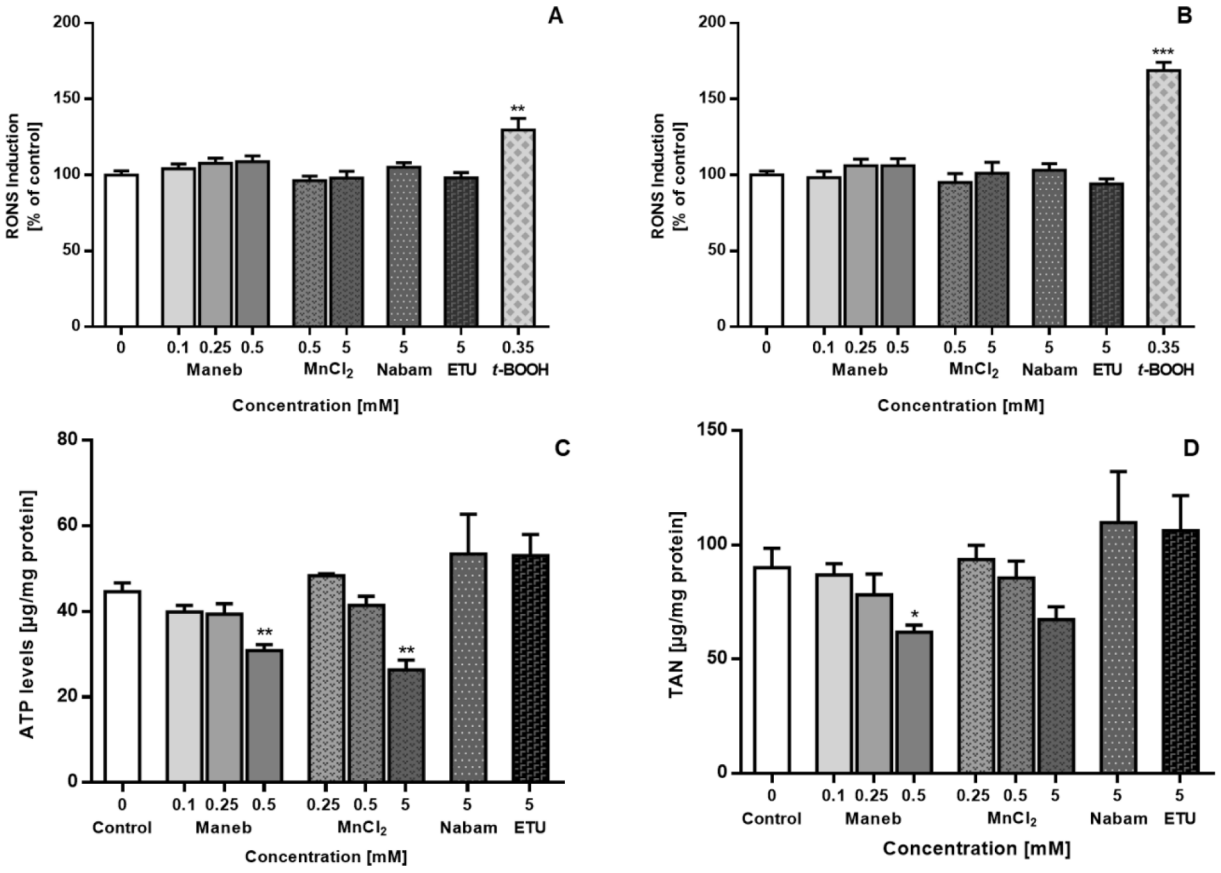

Fig. 6. **(A)** Fluorescence emission intensity normalized to respective control of wild-type worms (L1 larvae) after 30 min or 2 h **(B)** acute exposure to the individual species. 0.35 mM *t*-BOOH was used as a positive control. ATP levels **(C)** and TAN (**D**) were measured with LC-DAD and normalized to protein content following acute exposure for 2 h. Data are expressed as means ± SEM from at least three independent experiments. A one-way ANOVA with a Dunnett's multiple comparisons test was used for the statistical analysis. The following *p*-value summary was chosen: *p < 0.05, **p < 0.01, ***p < 0.001 compared to respective untreated control.

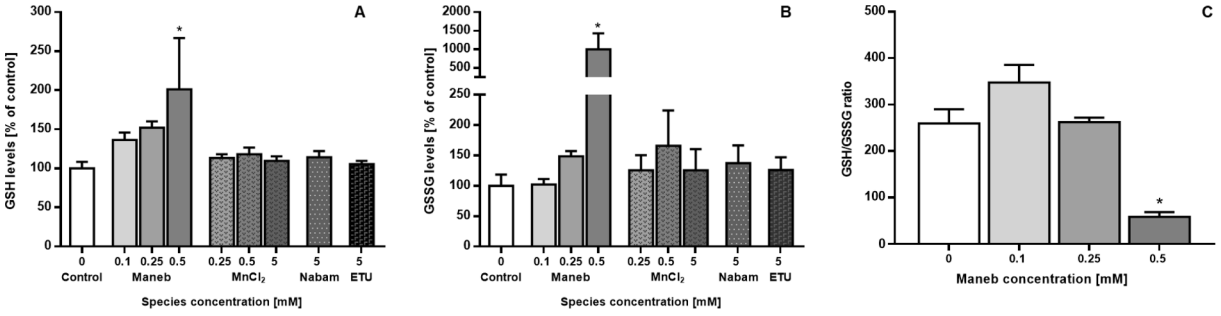

Fig. 7. **(A)** GSH amount measured with LC-MS/MS as GSH-NEM adduct normalized to protein content and normalized to respective control of wild-type worms (L1 larvae) following acute exposure for 2 h. **(B)** GSSG amount measured with LC-MS/MS normalized to protein content and normalized to respective control of wild-type worms (L1 larvae) following acute exposure for 2 h. **(C)** GSH/GSSG-ratio in L1-stage worms after exposure to Maneb for 2 h. Ratio was calculated by absolute data from each experiment (n = 3). Data are expressed as means ± SEM from at least three independent experiments. A one-way ANOVA with a Dunnett's multiple comparisons test was used for the statistical analysis. The following *p*-value summary was chosen: *p < 0.05 compared to respective untreated control.

quantification. In our study, we were able to detect GSSG levels in the picomolar range. Two *in vivo* zebrafish embryo studies found increased ROS levels and decreased GSH levels after 24 to 168 h exposure times (Paganotto Leandro et al., 2021; Da Costa-Silva et al., 2018). Pre-treatment (1 h) of the zebrafish embryos with the GSH precursor and antioxidant N-acetylcysteine (NAC) reduced the MZ-induced effects (Da Costa-Silva et al., 2018).

4. Conclusion

Maneb is often used as a part of resistance management strategies and is widely applied in Brazil, India, and China as a multi-site fungicide. However, epidemiological studies indicate an increased risk of neurodegenerative diseases associated with fungicide exposure, including Maneb. Since Maneb is postulated to degrade into several products under physiological conditions, this study aimed to learn more about the underlying mechanism through a direct comparison of the different species in one organism using advanced instrumental analytics. By using batches of our in-house synthesized pure Maneb, we could ensure that the effects of the fungicide were not caused by any impurities or additives which may be present in commercial products. This study showed that although Mn in Maneb is slightly less bioavailable than in $MnCl_2$,

Maneb is about eight times more toxic in *Caenorhabditis elegans*. For Maneb as underlying mechanisms of toxicity, oxidative stress and neurotoxicity could be identified. Neither $MnCl_2$ nor the metabolites of Maneb such as ETU could be identified as being responsible for Maneb toxicity. The structural analog of Maneb, the disodium salt Nabam, was significantly less toxic and caused no changes in glutathione or neurotransmitter levels. The ligand-controlled metal reactivity plays a critical role in the mechanism of neurotoxicity. Thus, the toxicity appears to be a combined effect of the organic backbone and the coordinated Mn ion.

Funding

This work was supported by the DFG Research Unit TraceAge (FOR 2558, BO4103/4–2).

CRediT authorship contribution statement

Laura Kubens: Conceptualization, Methodology, Formal analysis, Investigation, Data curation, Writing – original draft, Visualization. **Ann-Kathrin Weishaupt:** Conceptualization, Methodology, Writing – review & editing. **Vivien Michaelis:** Conceptualization, Methodology, Writing – review & editing. **Isabelle Rohn:** Writing – review & editing. **Fabian Mohr:** Conceptualization, Writing – review & editing, Supervision, Funding acquisition. **Julia Bornhorst:** Conceptualization, Funding acquisition, Project administration, Supervision, Writing – review & editing.

Declaration of competing interest

The authors declare that they have no known competing financial interests or personal relationships that could have appeared to influence the work reported in this paper.

Data availability

Data will be made available on request.

Acknowledgements

We thank the Caenorhabditis Genetics Center (CGC), funded by the NIH Office of Research Infrastructure Programs (P40 OD010440), for providing the *C. elegans* wild-type strain used in this work. We thank Micheal Aschner (Director, Einstein Center of Toxicology, Albert Einstein College of Medicine, New York) for the BY200 strain used in this work.

Appendix A. Supplementary data

Supplementary data to this article can be found online at https://doi.org/10.1016/j.envint.2023.108372.

Reference

Adeyemi, J.O., Onwudiwe, D.C., 2020. The mechanisms of action involving dithiocarbamate complexes in biological systems. Inorg. Chim. Acta 511, 119809. https://doi.org/10.1016/j.ica.2020.119809.

Andersen, J.K., 2004. Oxidative stress in neurodegeneration: cause or consequence? Nat. Med. 10 (Suppl. 7), S18–S25. https://doi.org/10.1038/nrn1434.

Anderson, C.C., Marentette, J.O., Rauniyar, A.K., Prutton, K.M., Khatri, M., Matheson, C., Reisz, J.A., Reigan, P., D'Alessandro, A., Roede, J.R., 2021. Maneb alters central carbon metabolism and thiol redox status in a toxicant model of Parkinson's disease. Free Radic. Biol. Med. 162, 65–76. https://doi.org/10.1016/j.freeradbiomed.2020.11.028.

Aschner, J.L., Aschner, M., 2005. Nutritional aspects of manganese homeostasis. Mol. Aspects Med. 26 (4–5), 353–362. https://doi.org/10.1016/j.mam.2005.07.003.

Aschner, M., Erikson, K.M., Herrero Hernández, E., Tjalkens, R., 2009. Manganese and its role in Parkinson's disease: from transport to neuropathology. NeuroMol. Med. 11 (4), 252–266. https://doi.org/10.1007/s12017-009-8083-0.

Baesler, J., Michaelis, V., Stiboller, M., Haase, H., Aschner, M., Schwerdtle, T., Sturzenbaum, S.R., Bornhorst, J., 2021. Nutritive Manganese and Zinc Overdosing in Aging C. elegans Result in a Metallothionein-Mediated Alteration in Metal Homeostasis. Mol. Nutr. Food Res. 65 (8), e2001176.

Barlow, B.K., Lee, D.W., Cory-Slechta, D.A., Opanashuk, L.A., 2005. Modulation of antioxidant defense systems by the environmental pesticide maneb in dopaminergic cells. Neurotoxicology 26 (1), 63–75. https://doi.org/10.1016/j.neuro.2004.07.004.

Bijwadia, S.R., Morton, K., Meyer, J.N., 2021. Quantifying Levels of Dopaminergic Neuron Morphological Alteration and Degeneration in Caenorhabditis elegans. J. Vis. Exp. 177 https://doi.org/10.3791/62894.

Bornhorst, J., Chakraborty, S., Meyer, S., Lohren, H., Brinkhaus, S.G., Knight, A.L., Caldwell, K.A., Caldwell, G.A., Karst, U., Schwerdtle, T., Bowman, A., Aschner, M., 2014. The effects of pdr1, djr1.1 and pink1 loss in manganese-induced toxicity and the role of α-synuclein in C. elegans. Metallomics : Integrated Biometal Science 6 (3), 476–490. https://doi.org/10.1039/c3mt00325f.

Brenner, S., 1974. The genetics of Caenorhabditis elegans. Genetics 77 (1), 71–94. https://doi.org/10.1093/genetics/77.1.71.

C. elegans Sequencing Consortium, 1998. Genome sequence of the nematode C. elegans: a platform for investigating biology. Science 282 (5396), 2012–2018.

Caldas, E.D., Miranda, M.C.C., Conceição, M.H., de Souza, L.C.K.R., 2004. Dithiocarbamates residues in Brazilian food and the potential risk for consumers. Food Chem. Toxicol. 42 (11), 1877–1883. https://doi.org/10.1016/j.fct.2004.07.006.

Calne, D.B., Chu, N.S., Huang, C.C., Lu, C.S., Olanow, W., 1994. Manganism and idiopathic parkinsonism: similarities and differences. Neurology 44 (9), 1583–1586. https://doi.org/10.1212/wnl.44.9.1583.

Camoni, I., Di Muccio, A., Pontecorvo, D., Citti, P., 1988. Survey of ethylenethiourea (ETU) in ethylenebis(dithiocarbamate) (EBDC) fungicides. Ecotoxicol. Environ. Saf. 16 (2), 176–179. https://doi.org/10.1016/0147-6513(88)90032-2.

Carmona, A., Roudeau, S., Perrin, L., Veronesi, G., Ortega, R., 2014. Environmental manganese compounds accumulate as Mn(II) within the Golgi apparatus of dopamine cells: relationship between speciation, subcellular distribution, and cytotoxicity. Metallomics : Integrated Biometal Science 6 (4), 822–832. https://doi.org/10.1039/c4mt00012a.

Carrasco Cabrera, L., Medina Pastor, P., 2022. The 2020 European Union report on pesticide residues in food. EFSA J. 20, (3). https://doi.org/10.2903/j.efsa.2022.7215.

Chen, P., Martinez-Finley, E.J., Bornhorst, J., Chakraborty, S., Aschner, M., 2013. Metal-induced neurodegeneration in C. elegans. Front. Aging Neurosci. 5, 18. https://doi.org/10.3389/fnagi.2013.00018.

Chen, P., Bornhorst, J., Diana Neely, M., Avila, D.S., 2018. Mechanisms and Disease Pathogenesis Underlying Metal-Induced Oxidative Stress. Oxid. Med. Cell. Longev. 2018, 7612172. https://doi.org/10.1155/2018/7612172.

Chen, S., Tran, S., Sigler, A., Murphy, T.H., 2011. Automated and quantitative image analysis of ischemic dendritic blebbing using in vivo 2-photon microscopy data. J. Neurosci. Methods 195 (2), 222–231. https://doi.org/10.1016/j.jneumeth.2010.12.018.

Costa-Silva, D.G.d., Leandro, L.P., Vieira, P.d.B., de Carvalho, N.R., Lopes, A.R., Schimith, L.E., Nunes, M.E.M., de Mello, R.S., Martins, I.K., de Paula, A.A., Cañedo, A.D., Moreira, J.C.F., Posser, T., Franco, J.L., 2018. N-acetylcysteine inhibits Mancozeb-induced impairments to the normal development of zebrafish embryos. Neurotoxicol. Teratol. 68, 1–12.

Costello, S., Cockburn, M., Bronstein, J., Zhang, X., Ritz, B., 2009. Parkinson's disease and residential exposure to maneb and paraquat from agricultural applications in the central valley of California. Am. J. Epidemiol. 169 (8), 919–926. https://doi.org/10.1093/aje/kwp006.

Cova, D., Fumagalli, P., Santagostino, A., 1991. Toxicity of Ethylene- bis -dithiocarbamates (EBDCs) in a Human Neuroblastoma Cell Line. Altern. Lab. Anim. 19 (1), 39–40. https://doi.org/10.1177/026119299101900108.

Domico, L.M., Zeevalk, G.D., Bernard, L.P., Cooper, K.R., 2006. Acute neurotoxic effects of mancozeb and maneb in mesencephalic neuronal cultures are associated with mitochondrial dysfunction. Neurotoxicology 27 (5), 816–825. https://doi.org/10.1016/j.neuro.2006.07.009.

Domico, L.M., Cooper, K.R., Bernard, L.P., Zeevalk, G.D., 2007. Reactive oxygen species generation by the ethylene-bis-dithiocarbamate (EBDC) fungicide mancozeb and its contribution to neuronal toxicity in mesencephalic cells. Neurotoxicology 28 (6), 1079–1091. https://doi.org/10.1016/j.neuro.2007.04.008.

Ferraz, H.B., Bertolucci, P.H., Pereira, J.S., Lima, J.G., Andrade, L.A., 1988. Chronic exposure to the fungicide maneb may produce symptoms and signs of CNS manganese intoxication. Neurology 38 (4), 550–553. https://doi.org/10.1212/wnl.38.4.550.

Fitzmaurice, A.G., Rhodes, S.L., Cockburn, M., Ritz, B., Bronstein, J.M., 2014. Aldehyde dehydrogenase variation enhances effect of pesticides associated with Parkinson disease. Neurology 82 (5), 419–426. https://doi.org/10.1212/WNL.0000000000000083.

Flenner, A.L., 1950. Manganous ethylene bis-dithiocarbamate and fungicidal compositions containing same. Assigned to E. I. du Pont de Nemours and Company. US-2504404.

Francis, P.T., Palmer, A.M., Snape, M., Wilcock, G.K., 1999. The cholinergic hypothesis of Alzheimer's disease: a review of progress. J. Neurol. Neurosurg. Psychiatry 66 (2), 137–147. https://doi.org/10.1136/jnnp.66.2.137.

Grosicka-Maciąg, E., Kurpios-Piec, D., Szumiło, M., Grzela, T., Rahden-Staroń, I., 2011. Protective effect of N-acetyl-L-cysteine against maneb induced oxidative and apoptotic injury in Chinese hamster V79 cells. Food Chem. Toxicol. 49 (4), 1020–1025. https://doi.org/10.1016/j.fct.2011.01.009.

Halliwell, B., 2006. Oxidative stress and neurodegeneration: where are we now? J. Neurochem. 97 (6), 1634–1658. https://doi.org/10.1111/j.1471-4159.2006.03907.x.

Harrison Brody, A., Chou, E., Gray, J.M., Pokyrwka, N.J., Raley-Susman, K.M., 2013. Mancozeb-induced behavioral deficits precede structural neural degeneration. Neurotoxicology 34, 74–81. https://doi.org/10.1016/j.neuro.2012.10.007.
Hester, W.F., Hill, D., 1943. Fungicidal composition. Assigned to Röhm & Haas Company. US-2317765.
Hoffman, L., Trombetta, L., Hardej, D., 2016. Ethylene bisdithiocarbamate pesticides Maneb and Mancozeb cause metal overload in human colon cells. Environ. Toxicol. Pharmacol. 41, 78–88. https://doi.org/10.1016/j.etap.2015.11.002.
Hogarth, G., 1978–2003.. Progress in Inorganic Chemistry 2005. Transition Metal Dithiocarbamates 53, 71–561.
Hornykiewicz, O., 2006. The discovery of dopamine deficiency in the parkinsonian brain. In: Parkinson's Disease and Related Disorders, Springer, Vienna, pp. 9–15.
Hurley, P.M., 1998. Mode of carcinogenic action of pesticides inducing thyroid follicular cell tumors in rodents. Environ. Health Perspect. 106 (8), 437–445. https://doi.org/10.1289/ehp.98106437.
International Agency for Research on Cancer, 1974. Some Anti-Thyroid and Related Substances, Nitrofurans and Industrial Chemicals. Supplement 7, 207–208.
Israeli, R., Sculsky, M., Tiberin, P., 1983. Acute central nervous system changes due to intoxication by Manzidan (a combined dithiocarbamate of Maneb and Zineb). Arch. Toxicol. Suppl. 6, 238–243. https://doi.org/10.1007/978-3-642-69083-9_43.
Kalia, L.V., Lang, A.E., 2015. Parkinson's disease. Lancet 386 (9996), 896–912. https://doi.org/10.1016/S0140-6736(14)61393-3.
Klöpping, H.L., van der Kerk, G.J.M., 1951. Investigations on organic fungicides: V. Chemical constitution and fungistatic activity of aliphatic bisdithiocarbamates and isothiocyanates. Recl. Trav. Chim. Pays-Bas 70 (11), 949–961. https://doi.org/10.1002/recl.19510701103.
Kubens, L., Truong, K.-N., Lehmann, C.W., Lützenkirchen-Hecht, D., Bornhorst, J., Mohr, F., 2023. The structure of Maneb: An important manganese-containing bis (dithiocarbamate) fungicide. Chem. A Eur. J. 29 (55), e202301721.
Kurttio, P., Savolainen, K., Naukkarinen, A., Kosma, V.M., Tuomisto, L., Penttilä, I., Jolkkonen, J., 1991. Urinary excretion of ethylenethiourea and kidney morphology in rats after continuous oral exposure to nabam or ethylenethiourea. Arch. Toxicol. 65 (5), 381–385. https://doi.org/10.1007/BF02284260.
Kurzatkowski, D.M., Trombetta, L.D., 2013. Maneb causes pro-oxidant effects in the hippocampus of Nrf2 knockout mice. Environ. Toxicol. Pharmacol. 36 (2), 427–436. https://doi.org/10.1016/j.etap.2013.04.016.
Leiphon, L.J., Picklo, M.J., 2007. Inhibition of aldehyde detoxification in CNS mitochondria by fungicides. Neurotoxicology 28 (1), 143–149. https://doi.org/10.1016/j.neuro.2006.08.008.
Leung, M.C.K., Williams, P.L., Benedetto, A., Au, C., Helmcke, K.J., Aschner, M., Meyer, J.N., 2008. Caenorhabditis elegans: an emerging model in biomedical and environmental toxicology. Toxicol. Sci.: Off. J. Soc. Toxicol. 106 (1), 5–28. https://doi.org/10.1093/toxsci/kfn121.
Liu, C., Liu, Z., Fang, Y., Liao, Z., Zhang, Z., Yuan, X., Yu, T., Yang, Y., Xiong, M., Zhang, X., Zhang, G., Meng, L., Zhang, Z., 2023. Exposure to dithiocarbamate fungicide maneb in vitro and in vivo: Neuronal apoptosis and underlying mechanisms. Environ. Int. 171, 107696 https://doi.org/10.1016/j.envint.2022.107696.
Martins, A.C., Gubert, P., Li, J., Ke, T., Nicolai, M.M., Moura, A.V., Bornhorst, J., Bowman, A.B., Aschner, M., 2022. Caenorhabditis elegans as a Model to Study Manganese-Induced Neurotoxicity. Biomolecules 12 (10). https://doi.org/10.3390/biom12101396.
McIntire, S.L., Jorgensen, E., Kaplan, J., Horvitz, H.R., 1993. The GABAergic nervous system of Caenorhabditis elegans. Nature 364 (6435), 337–341. https://doi.org/10.1038/364337a0.
Meco, G., Bonifati, V., Vanacore, N., Fabrizio, E., 1994. Parkinsonism after chronic exposure to the fungicide maneb (manganese ethylene-bis-dithiocarbamate). Scand. J. Work Environ. Health 20 (4), 301–305. https://doi.org/10.5271/sjweh.1394.
Mora, A.M., Córdoba, L., Cano, J.C., Hernandez-Bonilla, D., Pardo, L., Schnaas, L., Smith, D.R., Menezes-Filho, J.A., Mergler, D., Lindh, C.H., Eskenazi, B., van Wendel de Joode, B., 2018. Prenatal Mancozeb Exposure, Excess Manganese, and Neurodevelopment at 1 Year of Age in the Infants' Environmental Health (ISA) Study. Environmental health perspectives 126 (5), 57007. Doi: 10.1289/EHP1955.
Nass, R., Hall, D.H., Miller, D.M., Blakely, R.D., 2002. Neurotoxin-induced degeneration of dopamine neurons in Caenorhabditis elegans. PNAS 99 (5), 3264–3269. https://doi.org/10.1073/pnas.042497999.
Negga, R., Rudd, D.A., Davis, N.S., Justice, A.N., Hatfield, H.E., Valente, A.L., Fields, A. S., Fitsanakis, V.A., 2011. Exposure to Mn/Zn ethylene-bis-dithiocarbamate and glyphosate pesticides leads to neurodegeneration in Caenorhabditis elegans. Neurotoxicology 32 (3), 331–341. https://doi.org/10.1016/j.neuro.2011.02.002.
Negga, R., Stuart, J.A., Machen, M.L., Salva, J., Lizek, A.J., Richardson, S.J., Osborne, A. S., Mirallas, O., McVey, K.A., Fitsanakis, V.A., 2012. Exposure to glyphosate- and/or Mn/Zn-ethylene-bis-dithiocarbamate-containing pesticides leads to degeneration of γ-aminobutyric acid and dopamine neurons in Caenorhabditis elegans. Neurotox. Res. 21 (3), 281–290. https://doi.org/10.1007/s12640-011-9274-7.
Neumann, C., Baesler, J., Steffen, G., Nicolai, M.M., Zubel, T., Aschner, M., Bürkle, A., Mangerich, A., Schwerdtle, T., Bornhorst, J., 2020. The role of poly(ADP-ribose) polymerases in manganese exposed Caenorhabditis elegans. J. Trace Elem. Med. Biol. 57, 21–27. https://doi.org/10.1016/j.jtemb.2019.09.001.
Olanow, C.W., 2004. Manganese-induced parkinsonism and Parkinson's disease. Ann. N. Y. Acad. Sci. 1012, 209–223. https://doi.org/10.1196/annals.1306.018.
Paganotto Leandro, L., Siqueira de Mello, R., Da Costa-Silva, D.G., Medina Nunes, M.E., Rubin Lopes, A., Kemmerich Martins, I., Posser, T., Franco, J.L., 2021. Behavioral changes occur earlier than redox alterations in developing zebrafish exposed to Mancozeb. Environ. Pollut. 268 (Pt B), 115783 https://doi.org/10.1016/j.envpol.2020.115783.
Pereira, L., Kratsios, P., Serrano-Saiz, E., Sheftel, H., Mayo, A.E., Hall, D.H., White, J.G., LeBoeuf, B., Garcia, L.R. , Alon, U., Hobert, O., 2015. A cellular and regulatory map of the cholinergic nervous system of C. elegans. eLife 4. 10.7554/eLife.12432.
Peres, T.V., Arantes, L.P., Miah, M.R., Bornhorst, J., Schwerdtle, T., Bowman, A.B., Leal, R.B., Aschner, M., 2018. Role of Caenorhabditis elegans AKT-1/2 and SGK-1 in Manganese Toxicity. Neurotox. Res. 34 (3), 584–596. https://doi.org/10.1007/s12640-018-9915-1.
Printemps, N., Le Magueresse-Battistoni, B., Mhaouty-Kodja, S., Viguié, C., Michel, C., 2022. How to Differentiate General Toxicity-Related Endocrine Effects from Endocrine Disruption: Systematic Review of Carbon Disulfide Data. Int. J. Mol. Sci. 23 (6), 3153.
Roede, J.R., Jones, D.P., 2014. Thiol-reactivity of the fungicide maneb. Redox Biol. 2, 651–655. https://doi.org/10.1016/j.redox.2014.04.007.
Schon, E.A., Przedborski, S., 2011. Mitochondria: the next (neurode)generation. Neuron 70 (6), 1033–1053. https://doi.org/10.1016/j.neuron.2011.06.003.
Serrano-Saiz, E., Poole, R.J., Felton, T., Zhang, F., La Cruz, E.D. de, Hobert, O., 2013, Modular control of glutamatergic neuronal identity in C. elegans by distinct homeodomain proteins. Cell 155 (3), 659–673. 10.1016/j.cell.2013.09.052.
Singh, S., Brocker, C., Koppaka, V., Chen, Y., Jackson, B.C., Matsumoto, A., Thompson, D.C., Vasiliou, V., 2013. Aldehyde dehydrogenases in cellular responses to oxidative/electrophilic stress. Free Radic. Biol. Med. 56, 89–101. https://doi.org/10.1016/j.freeradbiomed.2012.11.010.
Smith, P.K., Krohn, R.I., Hermanson, G.T., Mallia, A.K., Gartner, F.H., Provenzano, M.D., Fujimoto, E.K., Goeke, N.M., Olson, B.J., Klenk, D.C., 1985. Measurement of protein using bicinchoninic acid. Anal. Biochem. 150 (1), 76–85. https://doi.org/10.1016/0003-2697(85)90442-7.
Soares, M.V., Viçozzi, G.P., Kuhn, E.C., Weishaupt, A.-K., Kubens, L., Bornhorst, J., Avila, D.S. Neurotoxicology of organic environmental toxicants using Caenorhabditis elegans as a model. In: Alternative Methods in Neurotoxicology Ed. J. B. Rocha, M. Aschner, L. G. Costa, Vol. 9, 149–180.
Sulston, J., Dew, M., Brenner, S., 1975. Dopaminergic neurons in the nematode Caenorhabditis elegans. J. Comp. Neurol. 163 (2), 215–226. https://doi.org/10.1002/cne.901630207.
Thiel, A., Weishaupt, A.-K., Nicolai, M.M., Lossow, K., Kipp, A.P., Schwerdtle, T., Bornhorst, J., 2023. Simultaneous quantitation of oxidized and reduced glutathione via LC-MS/MS to study the redox state and drug-mediated modulation in cells, worms and animal tissue. J. Chromatogr. B 1225, 123742.
Thind, T.S., Hollomon, D.W., 2018. Thiocarbamate fungicides: reliable tools in resistance management and future outlook. Pest Manag. Sci. 74 (7), 1547–1551. https://doi.org/10.1002/ps.4844.
Tuschl, K., Mills, P.B., Clayton, P.T., 2013. Manganese and the brain. Int. Rev. Neurobiol. 110, 277–312. https://doi.org/10.1016/B978-0-12-410502-7.00013-2.
U.S. Environmental Protection Agency, 1991. Ethylene thiourea (ETU); CASRN 96-45-7, Reference Dose for Oral Exposure (RfD). U.S. EPA. Online adress https://cfpub.epa.gov/ncea/iris2/chemicalLanding.cfm?substance_nmbr=239, last update 01.05.1991, Access date 13.10.2023.
van Wendel de Joode, B., Mora, A.M., Córdoba, L., Cano, J.C., Quesada, R., Faniband, M., Wesseling, C., Ruepert, C., Öberg, M., Eskenazi, B., Mergler, D., Lindh, C.H., 2014. Aerial application of mancozeb and urinary ethylene thiourea (ETU) concentrations among pregnant women in Costa Rica: the Infants' Environmental Health Study (ISA). Environ. Health Perspect. 122 (12), 1321–1328.
van Wendel de Joode, B.; Mora, A. M.; Lindh, C. H.; Hernández-Bonilla, D.; Córdoba, L.; Wesseling, C.; Hoppin, J. A.; Mergler, D., 2016. Pesticide exposure and neurodevelopment in children aged 6-9 years from Talamanca, Costa Rica. *Cortex* 85, 137–150. Doi: 10.1016/j.cortex.2016.09.003.
Vrábel, V., Gergely, Š., Lokaj, J., Kellö, E., Garaj, J., 1987. Structure of disodium ethylenebisdithiocarbamate hexahydrate. Acta Crystallogr. C 43 (12), 2293–2295. https://doi.org/10.1107/S0108270187088012.
Walker, F.O., 2007. Huntington's disease. Lancet 369 (9557), 218–228. https://doi.org/10.1016/S0140-6736(07)60111-1.
Weishaupt, A.-K., Kubens, L., Ruecker, L., Schwerdtle, T., Aschner, M., Bornhorst, J., 2023. A Reliable Method Based on Liquid Chromatography-Tandem Mass Spectrometry for the Simultaneous Quantification of Neurotransmitters in Caenorhabditis elegans. *Molecules* 28 (14). 10.3390/molecules28145373.
Wilson, D.M., Cookson, M.R., van den Bosch, L., Zetterberg, H., Holtzman, D.M., Dewachter, I., 2023. Hallmarks of neurodegenerative diseases. Cell 186 (4), 693–714. https://doi.org/10.1016/j.cell.2022.12.032.
Zeevalk, G.D., Derr-Yellin, E., Nicklas, W.J., 1995. Relative vulnerability of dopamine and GABA neurons in mesencephalic culture to inhibition of succinate dehydrogenase by malonate and 3-nitropropionic acid and protection by NMDA receptor blockade. J. Pharmacol. Exp. Ther. 275 (3), 1124–1130.
Zhou, Y., Shie, F.-S., Piccardo, P., Montine, T.J., Zhang, J., 2004. Proteasomal inhibition induced by manganese ethylene-bis-dithiocarbamate: relevance to Parkinson's disease. Neuroscience 128 (2), 281–291. https://doi.org/10.1016/j.neuroscience.2004.06.048.